연구논문

Journal of Drive and Control, Vol.19 No.1 pp.51-61 Mar. 2022
ISSN 2671-7972(print) ISSN 2671-7980(online)
http://dx.doi.org/10.7839/ksfc.2022.19.1.051

Backstepping Sliding Mode-based Model-free Control of Electro-hydraulic Systems

Hoai-Vu-Anh Truong[1], Hoai-An Trinh[1], Kyoung-Kwan Ahn[1*]

Received: 22 Nov. 2021, Revised: 24 Jan. 2022, Accepted: 30 Jan. 2022

Key Words : Backstepping control, Radial Basis Function, Electro-hydraulic system, Model-free control

Abstract: This paper presents a model-free system based on a framework of a backstepping sliding mode control (BSMC) with a radial basis function neural network (RBFNN) and adaptive mechanism for electro-hydraulic systems (EHSs). First, an EHS mathematical model was dedicatedly derived to understand the system behavior. Based on the system structure, BSMC was employed to satisfy the output performance. Due to the highly nonlinear characteristics and the presence of parametric uncertainties, a model-free approximator based on an RBFNN was developed to compensate for the EHS dynamics, thus addressing the difficulty in the requirement of system information. Adaptive laws based on the actor-critic neural network (ACNN) were implemented to suppress the existing error in the approximation and satisfy system qualification. The stability of the closed-loop system was theoretically proven by the Lyapunov function. To evaluate the effectiveness of the proposed algorithm, proportional-integrated-derivative (PID) and improved PID with ACNN (ACPID), which are considered two complete model-free methods, and adaptive backstepping sliding mode control, considered an ideal model-based method with the same adaptive laws, were used as two benchmark control strategies in a comparative simulation. The simulated results validated the superiority of the proposed algorithm in achieving nearly the same performance as the ideal adaptive BSMC.

1. Introduction

Taking the advantages of high load efficiency, high power-to-weight ratio, and fast response, electro-hydraulic systems (EHSs) are broadly applied for various high-order controlled systems such as construction machinery[1-5], robotic manipulators[6-7], automobile[8], crane[9], active suspension systems[10-11], brake system[12], and even in the field of renewable energy[13].

As prominent potential to extensively implement for automatic systems, HSs have triggered an upward trend in research to improve its workability of tracking performance under several specific conditions. Several studies of control have been carried out for this purpose. Lee et al.[14] applied a proportional-integrated-derivative (PID) controller for an electro-hydraulic servo system to exhibit the position tracking performance. Kim et al.[15] suggested using a feedback linearization integrated with disturbance observer to deal with existing uncertainties in the hydraulic system. Tran et al. proposed an adaptive backstepping sliding mode control (BSMC) with adaptive laws based on neural network to satisfy position tracking performance of hydraulic manipulator actuated by an electro-hydraulic system (EHS)[16]. Huh considered position control based on sliding mode approach for an EHS subjects to disturbance[17,18]. Truong et al. also proposed using backstepping control combined with extended state observer to cope with the hydraulic manipulator

* Corresponding author: kkahn@ulsan.ac.kr
1 School of Mechanical and Automotive Engineering, University of Ulsan, Daehak-ro 93, Nam-gu, Ulsan, Korea

behavior driven by the EHS in constrained motion[19]. Many studies of using advanced control strategies for industrial applications using EHSs were carried out with more improvement in system qualification reported. However, regarding the above literature, the system qualification is realized with the nominal system dynamics assumed to be prior known, which is hard to acquire in practice. Consequently, system dynamics and system parametric uncertainties are challenges to be address up to now.

RBFNN is known as a powerful tool to approximate any unknown smooth function with arbitrary accuracy in certain conditions. Therefore, this technique is widely developed for high-order and nonlinear complex systems to cope with system dynamics uncertainties. Yang et al.[20] employed adaptive RBFNN for robotic manipulator subjects to uncertain dynamics. Wu et al.[21] constructed an adaptive fault-tolerant control-based on RBFNN for nonlinear nonstrict-feedback systems. The RBFNN was employed to compensate for the system dynamics and unknown parametric uncertainties. Sun et al.[22] developed a novel finite-time control algorithm with the RBFNN, integrated to relax the system dynamics, for nonstrict-feedback systems to satisfy the output performance with the tracking error constraint required. Other reports of using the RBFNN for system dynamics compensation can be found in[23-26]. The effectiveness of the RBFNN was verified with the system output performance and its stability guaranteed via several simulations. However, from the representative studies in the literature, most works were conducted in which the system dynamics was partially well-determined, without considering the case of completely unknown system information. Thus, the contribution of using more RBFNN approximators to compensate for the system dynamics is still opened.

Although the RBFNN approximator can relax the system information, approximation error is inevitable due to the essential difference of model-free and model-based methods. Therefore, to enhance the system performance, adaptive laws are considerably involved to deal with redundant errors generated from approximation procedures. Theoretically, adaptive laws are designed to systematically adjust controller gains according to the system tracking error. Several attempts have been reported such as using additionally nonlinear function of error[27-28], NN back-propagation laws[29], or fuzzy logic control with designed rules[30] for controller gains adjustment to adopt with the requirement. Among various techniques, an actor-critic NN (ACNN) is more enhanced than conventional back-propagation and more generalization than the fuzzy, whose rules are heuristically formulated depending on a designer. This technique is a reinforced learning algorithm and can help learning a policy mapping inputs to output actions via parallel computing the agent's Advantage Function (TD error) or prediction error. The architecture of the ACNN consists of actor and critic processes in which the actor network chooses suitable actions at each time step while the critic network evaluates the quality of the given inputs state. Regarding this evaluation, the actor makes a decision to train the agent; thus, seeking out good state and avoid bad state. Wang et al.[31] applied the ACNN to seek out the suitable PID control gains. Kiumarsi et al.[32] developed an optimal control based on ACNN for nonlinear discreate-time systems to solve the system drift dynamics. Sun et al.[33] developed an adaptive PID-based reinforced learning ACNN to accomplish a tracking performance for a non-linear system and verified by a simulation on an inverted pendulum model.

Motivated from the above analysis, this paper aims to first-time propose an adaptive model-free BSMC-based RBFNN (BSM-RBF) to deal with the difficulty in system parameters identification and subsequently achieve the tracking performance for an electro-hydraulic pump-controlled system (EHPS). The contributions of the paper are as follows: First, the RBFNN is utilized to completely relax the unknown system dynamics. Then, the BSMC, known as strong robust and stabilizing controller against perturbations, is designed to achieve the system stability and robustness against unexpected perturbation. Moreover, an adaptive law based on ACNN technique is considerably developed to suppress the influence of the inevitable error from approximation process; thus, enhancing the system qualification in position tracking effort. The stability of the closed-loop system is theoretically achieved through Lyapunov theorem.

The rest of the paper is as follows: Section 2 dedicatedly describes the system dynamics of the EHPS. Then, the step-by-step proposed control strategy with the RBFNN and ACNN is presented in Section 3. Subsequently, Section 4 shows comparative simulations between the proposed control methodology with two other benchmark method, PID as a complete model-free control and conventional model-based BSMC, to verify the effectiveness of the proposed algorithm. Finally, worthy conclusions and potential for future development are discussed in Section 5.

2. System description

The simple architecture of electro-hydraulic pump-controlled system (EHPS) includes fixed displacement pump driven by an electric motor, two relief valves (rv_1 and rv_2), two check-valves (cv_1 and cv_2), and one actuator, a single-rod cylinder in this case, that is linked with a mass under the influence of external force as illustrated in Fig. 1. The movement of the cylinder, extraction and retraction to push or pull the mass, is controlled through adjusting the speed and rotation of the pump. The two relief valves are used for safety operation to protect the circuit in the case of over-pressure. The two check valves are equipped to compensate for the difference fluid between the two chambers or in the case when the pump cannot sufficiently supply fluid to the cylinder, the fluid will be drawn from the oil tank to supply for the cylinder.

2.1 System physical modeling

The movement of the mass interconnected with the cylinder is expressed as

$$m\ddot{x}+b_1\dot{x}+b_2 sign(x)+F_{ext}=P_1A_1-P_2A_2 \tag{1}$$

where $x, \dot{x}, \ddot{x}$ are position, velocity, and acceleration of the mass m, respectively; F is external force, b_1 and b_2 are coefficients of the unknown frictions; P_1 and P_2 are pressure in the bore-side (chamber-1) and rod-side (chamber-2) of the cylinder, respectively; and A_1 and A_2 are cross-section areas in the bore-side and rod-side of the cylinder, respectively.

2.2 Hydraulic modeling

The pressure P_1 and P_2 are generated as a result of from the hydraulic dynamics, run by the pump. The dynamics of the hydraulic circuit is derived as

$$\frac{dP_1}{dt}=\frac{\beta_e}{V_{10}+A_1x}\left(Q_{1in}-Q_{1out}-Q_{L1}\right) \tag{2}$$

$$\frac{dP_2}{dt}=\frac{\beta_e}{V_{20}+A_2\left(L-x\right)}\left(Q_{2in}-Q_{2out}-Q_{L2}\right) \tag{3}$$

where β_e is the effective bulk modulus of the oil; V_{10} and V_{20} are lumped initial volumes including initial volume in the two chamber and the volume of pipelines; Q_{1in} and Q_{1out} are inlet and outlet flow rates of the chamber-1, respectively; Q_{2in} and Q_{2out} are inlet and outlet flow rates of the chamber-1, respectively; Q_{L1} and Q_{L2} are unknown leakage flow rates in the two chambers; and L is the cylinder stroke.

The inlet and outlet flow rates of the chamber-1 is calculated by:

$$Q_{1in}=\eta D\omega+Q_{cv1} \tag{4}$$

$$Q_{2out}=A_1\dot{x}-Q_{rv1} \tag{5}$$

where D is the pump displacement; η is the volumetric efficiency of the pump; ω is the pump speed that is simplified as a proportional factor to the control signal, i.e., $\omega = K_{dr}u$ with K_{dr} being a proportional gain and u being a control signal; Q_{cv1} and Q_{rv1} are the flow rates through the check valve cv_1 and relief valve rv_1, respectively.

The modeling for the flow rates Q_{cv1} and Q_{rv1} are expressed as

$$Q_{cv1}=C_dA_{cv}\sqrt{\frac{2\left|P_t-P_1\right|}{\rho}} \tag{6}$$

$$Q_{rv1}=C_dA_{rv}\sqrt{\frac{2\left|P_1-P_t\right|}{\rho}} \tag{7}$$

where C_d is the discharge coefficient; A_{cv} and A_{rv} are the orifice area gradient of the check valves and relief valves, depending on the opening of the valves, respectively; ρ is the oil density; and P_t is oil tank pressure.

Similarly, the inlet and outlet flow rates of the chamber-1 is calculated by

$$Q_{1in} = A_2\dot{x} + Q_{cv2} \tag{8}$$

$$Q_{2out} = \eta D\omega + Q_{rv2} \tag{9}$$

where Q_{cv2} and Q_{rv2} are the flow rates through the check valve cv_2 and relief valve rv_2, respectively.

The modeling for the flow rates Q_{cv1} and Q_{rv1} are expressed as

$$Q_{cv2} = C_d\omega_{cv}\sqrt{\frac{2|P_t - P_2|}{\rho}} \tag{10}$$

$$Q_{rv1} = C_d\omega_{rv}\sqrt{\frac{2|P_2 - P_t|}{\rho}} \tag{11}$$

It is noteworthy that in the case of normal operation, i.e., no over-pressure occurs in the circuit, the dynamics of the relief valves can be ignored; thereby, the flow rates through these valves can consequently be ignored.

2.3 Entire system model

Let first define the system state variable as $x = [x_1, x_2, x_3]^T = [x, \dot{x}, (P_1A_1 - P_2A_2)]^T$. Then, regarding Eqs. (1) to (11), the whole system dynamics is rewritten as

$$\begin{cases} \dot{x}_1 = x_2 \\ \dot{x}_2 = f_2 + g_2x_3 \\ \dot{x}_3 = f_3 + g_3u \end{cases} \tag{12}$$

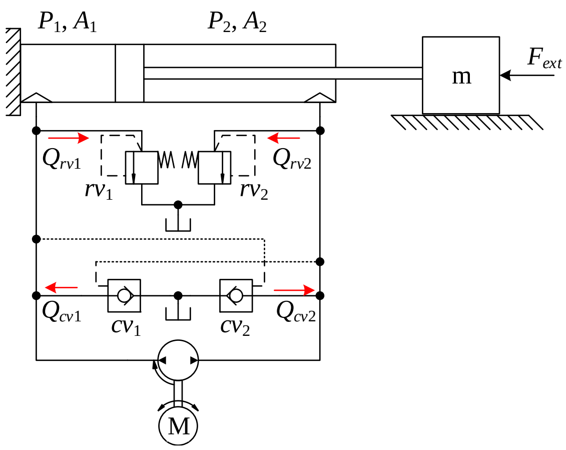

Fig. 1 Architecture of the EHPS system.

where $f_2 = -\frac{1}{m}\left(b_1\dot{x} + b_2 sign(x) + F_{ext}\right)$, $g_2 = \frac{1}{m}$,

$$f_3 = \frac{-\beta_e A_1^2 x_2}{V_{10} + A_1x_1} + \frac{-\beta_e A_2^2 x_2}{V_{20} + A_2(L - x_1)} - \frac{\beta_e A_1}{V_{10} + A_1x_1}Q_{L1} - \frac{\beta_e A_1}{V_{20} + A_2(L - x_1)}Q_{L2}$$

, $g_3 = \left(\frac{\beta_e A_1}{V_{10} + A_1x_1} + \frac{\beta_e A_1}{V_{20} + A_2(L - x_1)}\right)\eta DK$.

The friction inside and the specifications of the cylinder can be obtained from manual guide of manufacturer; however, the parameters of the hydraulic components are difficult to attain, such as the initial volumes, internal leakages, proportional gain, and orifice area gradient of valves. Then these parameters should be approximated to deal with the hydraulic dynamics.

3. Proposed Model-free Control Method

Regarding the difficulty in determining the hydraulic and internal system parameters, this section proposes the model-free method where the RBFNN is deployed to take place the information of the hydraulic characteristics with the Levant's differentiator integrated to obtain the cylinder velocity and a reinforced learning approach to adjust controller gains of the proposed ABSMC design for system qualification satisfaction.

3.1 Radial Basis Function Neural Network

The model of the hydraulic dynamics can be presented through the RBFNN as the followings:

$$\begin{cases} f_3 = W_f^{*T}\phi_f + \varepsilon_f \\ g_3 = W_g^{*T}\phi_g + \varepsilon_g \end{cases} \tag{13}$$

where W_{f3}^{*T} and W_{g3}^{*T} denote ideal constant vectors; ϕ_{f3} and ϕ_{g3} are radial basis function vectors regarding state variables.

For any radial basis function ϕ, it is identified by:

$$\phi = \exp\left(-\frac{(x - c_r)^T(x - c_r)}{2\mu^2}\right) \tag{14}$$

where x is a vector of input variables; c_r and μ are the vectors of center and width of the Gaussian functions, respectively.

Then, the system dynamics is rewritten as

$$\begin{cases} \dot{x}_1 = x_2 \\ \dot{x}_2 = f_2 + g_2 x_3 \\ \dot{x}_3 = \left(W_f^{*T}\phi_f + \varepsilon_f\right) + \left(W_g^{*T}\phi_g + \varepsilon_g\right)u \end{cases} \tag{15}$$

3.2 Levant's differentiator for velocity estimation

As the need of the cylinder velocity and acceleration in the backstepping process, the Levant's differentiator is employed to obtain these parameters without using necessary sensors and avoid the noise amplification generated from directly conventional differentiation of measured position. The estimator is defined as

$$\begin{cases} \hat{x}_1 = z_1,\ \dot{z}_1 = -\alpha_1 \left|z_1 - x_1\right|^{2/3} sign\left(z_1 - x_1\right) + z_2 \\ \dot{z}_2 = -\alpha_2 \left|z_2 - \dot{z}_1\right|^{1/2} sign\left(z_2 - \dot{z}_1\right) + z_3 \\ \dot{z}_3 = -\alpha_3 sign\left(z_3 - \dot{z}_2\right) \end{cases} \tag{16}$$

where α_1, α_2, and α_3 are designed positive constants; z_1, z_2, and z_3 are estimations of $x, \dot{x}, \ddot{x}$, respectively. The convergence of the estimated variables to the real values is achieved by suitably adopting values of λ_1, λ_2, and λ_3. According to[34], the Levant's differentiator can help to achieve finite time convergence of the estimation regardless the control input. Hence, the proposed control strategy can be developed separately with the full variables available.

3.3 Proposed control algorithm and stability proof

In this section, the backstepping sliding mode control is step-by-step designed. The proposed control scheme is illustrated in Fig. 2. To facilitate the control design, the following assumptions are introduced:

Assumption 1: The system parametric uncertainties are unknown but bounded, and their derivative are also bounded.

Assumption 2: Regarding the hardware signals saturation, the control input, pressures inside the circuit, and cylinder response are saturated. The problems of input saturation and output constraint are temporarily ignored in this study.

Firstly, let define the state error of $e_1 = x_1 - x_{1d}$, $e_2 = \dot{e}_1 = x_2 - \dot{x}_{1d}$, $e_3 = x_3 - x_{3d}$.

Step 1:

Define the sliding surface:

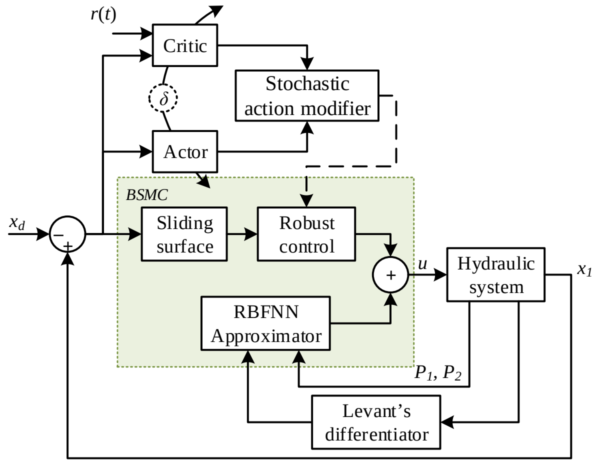

Fig. 2 Proposed control scheme for the EHPS system.

$$s = e_2 + \lambda e_1 \tag{17}$$

with λ is the slope of the sliding manifold.

Choose the Lyapunov candidate V_1 as

$$V_1 = \frac{1}{2}s^2 \tag{18}$$

Taking derivative V_1 yields:

$$\begin{aligned} \dot{V}_1 &= s\dot{s} \\ &= s^T\left(\dot{e}_2 + \lambda e_2\right) \\ &= s\left(f_2 + g_2\left(e_3 + x_{3d}\right) - \ddot{x}_{1d} + \lambda \dot{e}_1\right) \end{aligned} \tag{19}$$

Then, the virtual desired force for the actuator dynamics is chosen as

$$x_{3d} = \frac{1}{g_2}\left(-f_2 + \ddot{x}_{1d} - \lambda \dot{e}_1 - K_s s - \eta_s \tanh\left(\frac{s}{\delta}\right)\right) \tag{20}$$

where K_s and η_s are control gains, δ is an arbitrarily small constant.

Substituting the virtual control to Eq. (19) results in:

$$\dot{V}_1 = -K_s s^2 - \eta_s s \tanh\left(s/\delta\right) + g_2 s e_3 \tag{21}$$

As can be seen, the Lyapunov V_1 is affected by the term $g_2 s e_3$, which associates with the hydraulic dynamics. Then, a control law in the hydraulic inner loop should be designed such that the force tracking error is suppressed; thus, the derivative V_1 becomes semi-negative definite and the sliding surface s_1 will converge to zero.

Step 2:

Choose the Lyapunov candidate V_2 as

$$V_2 = V_1 + \frac{1}{2}e_3^2 + \frac{1}{2\gamma_f}\tilde{W}_f^T\tilde{W}_f + \frac{1}{2\gamma_g}\tilde{W}_g^T\tilde{W}_g \tag{22}$$

where $\tilde{W}_f = W_f^* - \hat{W}_f$, $\tilde{W}_g = W_g^* - \hat{W}_g$, $\hat{W}_f$ and $\hat{W}_g$ are estimated vectors of W_{f3}^* and W_{g3}^*, γ_{f3} and γ_{g3} are constants.

Taking derivative V_2 yields:

$$\begin{aligned}\dot{V}_2 &= -K_1 s^2 - \eta_1 s\tanh\left(s/\delta\right) + g_2 s e_3 + e_3\left(f_3 + g_3 u - \dot{x}_{3d}\right)\\ &\quad - \frac{1}{\gamma_f}\tilde{W}_f^T\dot{\hat{W}}_f - \frac{1}{\gamma_g}\tilde{W}_g^T\dot{\hat{W}}_g\end{aligned} \tag{23}$$

$$\begin{aligned}\Leftrightarrow \dot{V}_2 &= -K_1 s^2 - \eta_1 s\tanh\left(s/\delta\right) + g_2 s e_3\\ &\quad + e_3\left(f_3 + \tilde{g}_3 u + \hat{g}_3 u - \dot{x}_{3d}\right)\\ &\quad - \frac{1}{\gamma_f}\tilde{W}_f^T\dot{\hat{W}}_f - \frac{1}{\gamma_g}\tilde{W}_g^T\dot{\hat{W}}_g\end{aligned} \tag{24}$$

Regarding Eq. (24), to obtain the ideal results where the system dynamics is completely compensated, the control input signal u and adaptive laws for estimated term $\hat{W}_f$ and $\hat{W}_g$ are designed by:

$$u = \frac{1}{\hat{g}_3}\left(-\hat{f}_3 + \dot{x}_{3d} - g_2 s - K_3 e_3 - \eta_3 sign\left(e_3\right)\right) \tag{25}$$

$$\dot{\hat{W}}_f = \gamma_f e_3 \phi_f - \xi_f \hat{W}_f \tag{26}$$

$$\dot{\hat{W}}_g = \gamma_g e_3 \phi_g u - \xi_g \hat{W}_g \tag{27}$$

Substituting the control input in Eq. (25) and adaptive laws (26), (27) into Eq. (24) results in:

$$\begin{aligned}\dot{V}_2 &= -K_1 s^2 - \eta_1 s\tanh\left(s/\delta\right) - K_3 e_3^2 - \eta_3 e_3 sign\left(e_3\right)\\ &\quad + e_3\varepsilon_f + \frac{1}{\gamma_f}\xi_f\tilde{W}_f^T\hat{W}_f + e_3\varepsilon_g u + \frac{1}{\gamma_g}\xi_g\tilde{W}_g^T\hat{W}_g\end{aligned} \tag{28}$$

$$\begin{aligned}\dot{V}_2 &= -K_1 s^2 - \eta_1 s\tanh\left(s/\delta\right) - K_3 e_3^2 - \eta_3 e_3 sign\left(e_3\right)\\ &\quad - \frac{\xi_f}{\gamma_f}\tilde{W}_f^T\tilde{W}_f - \frac{\xi_g}{\gamma_g}\tilde{W}_g^T\tilde{W}_g\\ &\quad + e_3\varepsilon_f + \frac{1}{\gamma_f}\xi_f\tilde{W}_f^T W_f + e_3\varepsilon_g u + \frac{1}{\gamma_g}\xi_g\tilde{W}_g^T W_g\end{aligned} \tag{29}$$

It is noteworthy that the control signal u is saturated by $|u| \le u_{\max}$ due to the driver and system characteristics. Hence, applying Young's inequality for Eq. (29) yields:

$$\begin{aligned}\dot{V}_2 &\le -K_1 s^2 - \eta_1 s\tanh\left(s/\delta\right) - K_3 e_3^2 - \eta_3 e_3 sign\left(e_3\right)\\ &\quad - \frac{\xi_f}{\gamma_f}\tilde{W}_f^T\tilde{W}_f - \frac{\xi_g}{\gamma_g}\tilde{W}_g^T\tilde{W}_g\\ &\quad + \left(\frac{1}{2}e_3^2 + \frac{1}{2}\varepsilon_f^2\right) + \frac{\xi_f}{\gamma_f}\left(\frac{1}{2}\tilde{W}_f^T\tilde{W}_f + \frac{1}{2}W_f^T W_f\right)\\ &\quad + \left(\frac{1}{2}e_3^2 + \frac{1}{2}\varepsilon_g^2\right)u_{\max} + \frac{\xi_g}{\gamma_g}\left(\frac{1}{2}\tilde{W}_g^T\tilde{W}_g + \frac{1}{2}W_g^T W_g\right)\end{aligned} \tag{30}$$

$$\dot{V}_2 \le -aV_2 + \Gamma \tag{31}$$

Then, the proposed algorithm is concluded to be uniformly ultimately bounded.

3.4 Actor critic NN for gain-scheduling

In this section, the adaptive law based on reinforced learning ACNN is dedicatedly derived for the controller gains adjustment. The control architecture of the ACNN is depicted in Fig. 3 with critic, actor, and stochastic action modifier (SAM) processes.

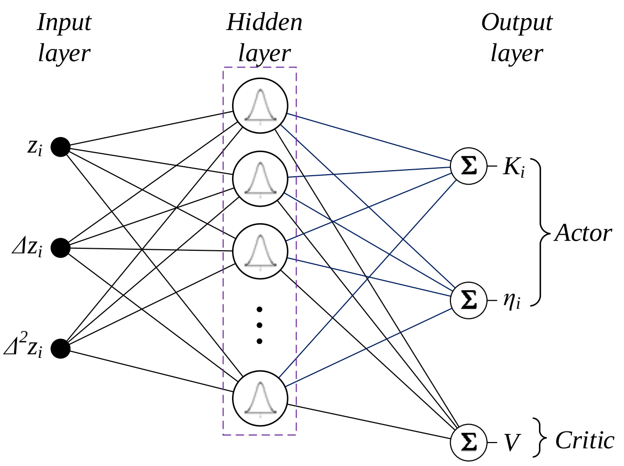

Fig. 3 Architecture of the Actor-Critic NN.

The Actor process is used to estimate a policy function and realize the mapping from the current system state vector to the recommended controller gains $\Delta K(t)$ and $\Delta\eta(t)$. The Critic process receives a system state vector and an external reinforcement signal from the environment and produces a TD error $\delta_{TD}(t)$ and an estimated value function $V(t)$. The SAM is used to stochastically generate the actual control gains $K(t)$ and $\eta(t)$ regarding the recommended parameter $\Delta K(t)$ and $\Delta\eta(t)$ suggested by the Actor and the estimated signal $V(t)$ from the Critic.

As shown in Fig. 3, each of Actor or Critic process includes input layer, hidden layer, and output layer. The input layer assigns tracking error, its change rate and its acceleration as inputs, for both actor and critic neural networks. The output of the critic network is the evaluation function, here in this paper is defined as $V(t)$, and the actor network returns the adjustable controller gains.

For the sake of simplicity, let define $z_i = x_i - x_{id}$, with i =1,2 being the step i^{th} in the BSMC process, i.e., if i=1, then $z_1 = x_1 - x_{1d}$, if i=2, then $z_2 = x_3 - x_{3d}$. The outputs of the actor network are ΔK_i and $\Delta\eta_i$, and the output of the critic networks is $V_i(t)$.

Define an input vector $X_i = [z_i(t);\ \Delta z_i(t);\ \Delta^2 z_i(t)]^T$ with $\Delta z_i(t)=z_i(t)-z_i(t-1)$, $\Delta^2 z_i(t)=z_i(t)-2z_i(t-1)+z_i(t-2)$.

The Kernel function in the hidden layer is expressed by:

$$\phi_j(t)=\exp\left(\frac{-\left\|X(t)-\mu_{ij}\right\|^2}{2\sigma_{ij}^2}\right) \tag{32}$$

where j is a number of nodes in the hidden layer, μ_{ij} is the center of node j^{th} in the step i^{th}, and σ_{ij} is the standard deviation of node j^{th} in step i^{th}.

The outputs of the Actor and Critic NNs are:

$$\begin{cases}\Delta K_{jk}=\sum_{j=1}^{k}W_{ijk}(t)\phi_j(t)\\ V_i(t)=\sum_{j=1}^{k}V_{ijk}(t)\phi_j(t)\end{cases} \tag{33}$$

where k=1,2; ΔK_{ik} is adjusted gains of: K (for k=1) and η (for k=2) of step i^{th}; W_{ijk} is a weighting factor of output k^{th} from node j^{th} of step i^{th} in the Actor NN, V_{ijk} is a weighting factor of output k^{th} from node j^{th} of step i^{th} in the Critic NN.

Then the adaptive control gains are obtained by:

$$\begin{cases}K_i=K_{i,0}+\Delta K_i+\xi\left(0,\dfrac{1}{1+\exp\left(2V(t)\right)}\right)\\ \eta_i=\eta_{i,0}+\Delta\eta_i+\xi\left(0,\dfrac{1}{1+\exp\left(2V(t)\right)}\right)\end{cases} \tag{34}$$

with ξ is Gaussian distribution with mean 0, covariance $1/(1+\exp(2V(t)))$.

The updating laws for weighting factors W_{ijk} and V_{ijk} are implemented through TD error, δ_{TD}, evaluation induced from the Critic process as

$$\begin{cases}\delta_{TD}(t)=r(t)+\gamma V(t+1)-V(t)\\ r(t)=\alpha r_e(t)+\beta r_{ec}(t),\begin{cases}r_e(t)=\begin{cases}0 & |z_i(t)|\le\varepsilon_i\\ -0.5 & otherwise\end{cases}\\ r_e(t)=\begin{cases}0 & |z_i(t)|\le|z_i(t-1)|\\ -0.5 & otherwise\end{cases}\end{cases}\\ \gamma\in[0,1]\end{cases} \tag{35}$$

and

$$\begin{cases}W_{ijk}(t+1)=W_{ijk}(t)+\zeta_A\delta_{TD}(t)\dfrac{K_{ik}(t)-\Delta K_{ik}(t)}{\sigma_{ij}(t)}\phi_j(t)\\ V_{ijk}(t+1)=V_{ijk}(t)+\zeta_C\delta_{TD}(t)\phi_j(t)\\ \mu_{ij}(t+1)=\mu_{ij}(t)+\zeta_\mu\delta_{TD}(t)V_{ijk}(t)\phi_j(t)\dfrac{X_i(t)-\mu_{ij}(t)}{\sigma i_j^2}\\ \sigma_{ij}(t+1)=\sigma_{ij}(t)+\zeta_\sigma\delta_{TD}(t)V_{ijk}(t)\phi_j(t)\dfrac{\left\|X_i(t)-\mu_{ij}(t)\right\|}{\sigma i_j^3}\end{cases} \tag{36}$$

where ζ_A, ζ_C, ζ_μ, ζ_σ are learning rates for updating weighting factors, center and standard deviation of the Gaussian Kernel function, respectively.

4. Simulations

To verify the effectiveness of the proposed control algorithm, other three controllers of PID, ACNN PID (ACPID), and adaptive BSMC are involved as benchmarks on the EHPS, whose parameters are described in Table 1. The other existing model-free approaches are not considered in the comparison due to the different problems considered. The PID and ACPID controllers are involved as completely model-free methods without hydraulic dynamics consideration whereas the adaptive BSMC, conducted based on conventional BSMC and the same adaptive law of the ACNN, is a model-based method with completely known system parameters, including hydraulic dynamics.

The aim is that the proposed algorithm is expected to exhibit better performance in comparison with complete model-free and asymptotically perform as same as the model-based method.

Table 1 EHPS' parameters

Parameters	Values	Unit
m	50	[kg]
b_1 b_2	1 258	[N/m/s] [N]
β_e	5.34x10^{8}	[Pa]
D_1	0.04	[m]
D_2	0.028	[m]
V_{10}	4.375x10^{-4}	[m^3]
V_{20}	2.88x10^{-4}	[m^3]
L	0.5	[m]
D	5.83x10^{-7}	[m^3/rad]
K_{dr}	10π	[rad/s/V]

Table 2 Controllers' parameters

Controller	Values
PID	K_P = 500; K_I = 200; K_D = 1
ACNNPID	$K_{P,0}$ = 500; $K_{I,0}$ = 200; K_D = 1 ACNN: i = 3; j = 5; k = 2; μ_{init} = 2xeyes(3,5); σ_{init} = 0.5x eyes(3,5); W_{init} = 10xeyes(5,2); V_{init} = 5xeyes(5,1); ζA = ζC = 0.5; ζ_μ = ζ_σ = 0.2; ε = 0.05
BSMC	λ = 10; Ks = 50; ηs = 0.05; $K3$ = 50; $\eta 3$ = 0.001; δ = 10–5
Proposed controller	BSMC initial gains: $Ks_{,0}$ = 50; $\eta s_{,0}$ = 0.05; $K3,0$ = 50; $\eta 3,0$ = 0.001; δ = 10–5 RBFNN: γf = 0.5; γg = 0.5; ξf = 0.5; ξg = 0.5 Levant's differentiator: $\alpha 1$ = 5; $\alpha 2$ = 10; $\alpha 3$ = 5 ACNN: i = 3; j = 5; k = 2; μ_{init} = 2xeyes(3,5); σ_{init} = 0.5x eyes(3,5); W_{init} = 10xeyes(5,2); V_{init} = 5xeyes(5,1); ζA = ζC = 0.5; ζ_μ = ζ_σ = 0.2; ε = 0.05

For fair comparison, the nominal switching control gains of both proposed controller and BSMC are set as the same as each other. The PID control gains are tuned such that the best performance can be exhibited. The values of all controllers are presented in Table 2. The simulation was implemented by using MATLAB environment, version 2020a with the fixed-step sampling time of 0.1 ms and the ODE-4 (Runge-Kutta solver) used.

The reference trajectory is sinusoidal function of:

$$x_{1d} = 0.25 + 0.15\sin(\pi t/5)\ \text{(m)} \tag{37}$$

The tracking performance of the examined EHS under three controllers is depicted in Fig. 4, in which the black line denotes the desired reference trajectory whereas the dot-green line, the dashed-blue line, the dot-dashed-purple line, and the dot-dashed-red line present the system tracking effort under the PID, the ACPID, the adaptive BSMC, and the proposed control methodology, respectively.

The tracking error under three control strategies is displayed in Fig. 5. As can be seen from the comparative simulations, the adaptive BSMC exhibited the best performance with the smallest tracking error, in the range of ±0.01 (m), due to the system dynamics completely compensated.

The model-free PID undoubtedly returned the worst performance with the largest tracking error due to the influence of the system dynamics.

The ACPID could achieve a better performance in comparison with the PID. However, the ignorance of system dynamics caused the tracking performance to fluctuate regardless of adding the ACNN adaptive laws.

On the contrary, the proposed methodology achieved the nearly same as the benchmark BSMC with the tracking error varying in the range of ±0.008 (m) without fluctuation.

5. Conclusion

This paper presented an adaptive model-free BSM-RBF control for the EHS to solve the difficulty in highly nonlinear system and then achieve position tracking performance. The existing problem of system

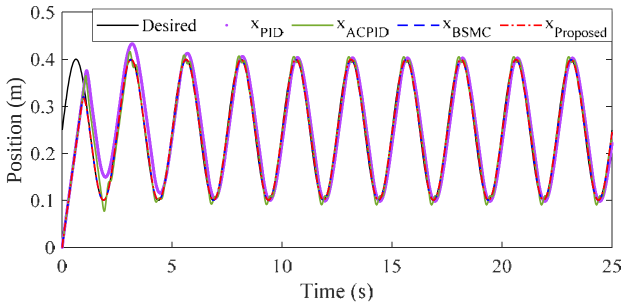

Fig. 4 Tracking performance under four controllers.

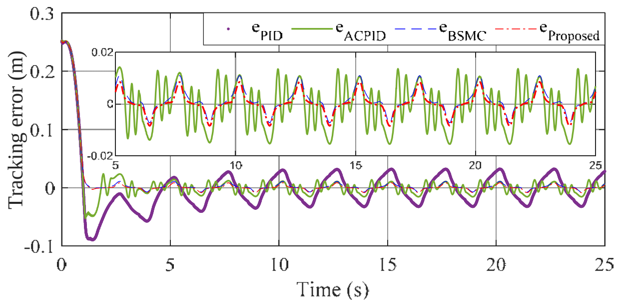

Fig. 5 Tracking errors under four controllers.

dynamics and parametric uncertainties were addressed by using the RBFNN approximator with the Levant's differentiator considered to obtain unmeasured signal of velocity. Then the proposed BSM-RBF control was formulated with adaptive law developed based on the ACNN technique to adopt with the system behavior. The stability of the closed-loop system is guaranteed through Lyapunov proof. The comparative simulation result with the other two benchmarks evidently indicated the superior effectiveness of the proposed algorithm. However, the existing shortcomings of input saturation and output constraint are not included in this regard. Due to the significant influences when implementing on real physical systems, these problems will be clarified in the next research.

As the prominent potential of the EHSs for industrial applications and shortcoming of model-free control improvement, this paper can be considered as a premise for further development with more advanced and integrated techniques.

Acknowledgement

This results was supported by "Regional Innovation Strategy (RIS)" through the National Research Foundation of Korea(NRF) funded by the Ministry of Education(MOE)(2021RIS-003).

Conflicts of Interest

The authors declare that there is no conflict of interest.

References

1) Y. C. Kwon et al., "Development of the HPM System to Improve Efficiency of the Hydraulic Excavator," Journal of Drive and Control, Vol.16, No.4, pp.1-8, 2019.
2) Y.-H. Im et al., "Real-Time Simulation of an Excavator Considering the Functional Valves of the MCV," Journal of Drive and Control, Vol.16, No.4, pp.38-47, 2019.
3) H. Yun and S. Kim, "A Study on Cycle Time and Power Saving Effect of a Hydraulic Hybrid Injection Molding Machine using a Servo Motor," Journal of Drive and Control, Vol.17, No.3, pp.15-25, 2020.
4) H. Yun and S. Kim, "A Study on Cycle Time and Power Saving Effect of a Hydraulic Hybrid Injection Molding Machine using a Servo Motor," Journal of Drive and Control, Vol.17, No.3, pp.15-25, 2020.
5) Y. S. Park et al., "A Study on the Regeneration Efficiency of the Electric Forklift Using the Variable Hydraulic Motor," Journal of Drive and Control, Vol.17, No.3, pp.26-32, 2020.
6) Y. T. Cha, Y. H. Lee and S. J. Choi, "Implementation of Virtual Environment System for Multi-joint Manipulator Designed for Special Purpose Equipment with Wearable Joystick used in Disaster Response," Journal of Drive and Control, Vol.17, No.3, pp.33-46, 2020.
7) J. T. Kim et al., "Control Strategy and Verification of Dual-Arm Manipulator for Disaster-Responding Special Purpose Machinery," Journal of Drive and Control, Vol.17, No.4, pp.31-37, 2020.
8) S. Y. Noh and J. S. Jang, "Analysis Model Development and Sensitivity Analysis of an

Independent Driving System for Disaster Response," Journal of Drive and Control, Vol.17, No.4, pp.38-45, 2020.

9) S.-H. Ko, K.-H. Lee and C.-H. Lee, "Safety Verification of Gantry Cranes using Hydraulic Cylinders," Journal of Drive and Control, Vol.16, No.2, pp.8-14, 2019.

10) H. M. Moon et al., "Active Vibration Control of Three-Stage Mast of Reach Truck," Journal of Drive and Control, Vol.16, No.3, pp.1-7, 2019.

11) M. S. Chang et al., "Analysis of a Variable Damper and Pneumatic Spring Suspension for Bicycle Forks using Hydraulic-Pneumatic Circuit Model," Journal of Drive and Control, Vol.16, No.1, pp.7-13, 2019.

12) S. Yoo et al., "Position Sensorless Control of PMSM Drive for Electro-Hydraulic Brake Systems," Journal of Drive and Control, Vol.16, No.3, pp.23-32, 2019.

13) H. T. Do et al., "Maximum Power Point Tracking and Output Power Control on Pressure Coupling Wind Energy Conversion System," IEEE Transactions on Industrial Electronics, vol. 65, No. 2, pp.1316-1324, 2018.

14) S. J. Lee et al., "Modeling and PID Control of an Electro-Hydraulic Servo System," Journal of Drive and Control, Vol.16, No.4, pp.16-22, 2019.

15) T.-H. Kim, I.-Y. Lee and J.-S. Jang, "Hydraulic Control System Using a Feedback Linearization Controller and Disturbance Observer - Sensitivity of System Parameters－, Journal of Drive and Control, Vol.16, No.2, pp.59-65, 2019.

16) D. T. Tran, H. V. A. Truong and K. K. Ahn, "Adaptive Backstepping Sliding Mode Control Based RBFNN for a Hydraulic Manipulator Including Actuator Dynamics," Applied Sciences, Vol. 9, 2019.

17) J. Y. Huh, "Position Control of an Electro-hydraulic Servo System with Sliding Mode," Journal of Drive and Control, Vol.18, No.3, pp.16-22, 2021.

18) J. Y. Huh, "Position Control of an Electro-hydraulic Servo System with Disturbance," Journal of Drive and Control, Vol.18, No.3, pp.1-7, 2021.

19) H. V. A. Truong et al., "A Robust Observer for Sensor Faults Estimation on n-DOF Manipulator in Constrained Framework Environment," IEEE Access, Vol. 9, pp.88439-88451, 2021.

20) R. Yang et al., "Discrete-time Optimal Adaptive RBFNN Control for Robot Manipulators with Uncertain Dynamics, " Neurocomputing, Vol. 234, pp.107-115, 2017.

21) C. Wu et al., "Observer-Based Adaptive Fault-Tolerant Tracking Control of Nonlinear Nonstrict-Feedback Systems," IEEE Transactions on Neural Networks and Learning Systems, vol. 29, No. 7, July 2018.

22) K. Sun et al., "A Novel Finite-Time Control for Nonstrict Feedback Saturated Nonlinear Systems With Tracking Error Constraint," IEEE Transactions on Systems, Man, and Cybernetics: Systems, Vol. 51, No. 6, June 2021.

23) Y. Pan and H. Yu, "Biomimetic Hybrid Feedback Feedforward Neural-Network Learning Control," IEEE Transactions on Neural Networks and Learning Systems, Vol. 28, No. 6, pp.1481-1487, 2017.

24) L. Ortombina, F. Tinazzi and M. Zigliotto, "Adaptive Maximum Torque per Ampere Control of Synchronous Reluctance Motors by Radial Basis Function Networks," IEEE Journal of Emerging and Selected Topics in Power Electronics, Vol. 7, No. 4, pp.2531-2539, 2019.

25) Z. Hewei and L. Rui, "Typical Adaptive Neural Control for Hypersonic Vehicle Based on Higher-order Filters," Journal of Systems Engineering and Electronics, Vol. 31, No. 5, pp. 1031-1040, 2020.

26) L. Ma and L. Liu, "Adaptive Neural Network Control Design for Uncertain Nonstrict Feedback Nonlinear System with State Constraints," IEEE Transactions on Systems, Man, and Cybernetics: Systems, Vol. 51, No. 6, pp.3678-3686, 2021.

27) M. Van, S. S. Ge and H. Ren, "Robust Fault-Tolerant Control for a Class of Second-Order Nonlinear Systems Using an Adaptive Third-Order Sliding Mode Control," IEEE Transactions on

Systems, Man, and Cybernetics: Systems, Vol. 47, No. 2, pp.221-228, 2017.
28) S. D. Nguyen, S.-B. Choi and T.-I. Seo, "Adaptive Fuzzy Sliding Control Enhanced by Compensation for Explicitly Unidentified Aspects," International Journal of Control, Automation and Systems, Vol. 15, No. 6, pp.2906-2920, 2017.
29) H. V. A. Truong, D. T. Tran and K. K. Ahn, "A Neural Network Based Sliding Mode Control for Tracking Performance with Parameters Variation of a 3-DOF Manipulator," Applied Sciences, Vol. 9(2023), 2019.
30) H. V. A. Truong et al., "Adaptive Fuzzy Backstepping Sliding Mode Control for a 3-DOF Hydraulic Manipulator with Nonlinear Disturbance Observer for Large Payload Variation," Applied Sciences, Vol. 9(3290), 2019.
31) X. Wang, Y, Cheng and W. Sun, "A Proposal of Adaptive PID Controller Based on Reinforcement Learning," Journal of China University of Mining & Technology, Vol 17, No. 1, pp.40-44, 2007.
32) B. Kiumarsi and F. L. Lewis, "Actor–Critic-Based Optimal Tracking for Partially Unknown Nonlinear Discrete-Time Systems," IEEE Transactions on Neural Networks and Learning Systems, Vol. 26, No. 1, 2015.
33) Q. Sung, C. Du, Y. Duan, H. Ren and H. Li, "Design and application of adaptive PID controller based on asynchronous advantage actor–critic learning method," Wireless Networks, Vol. 27, pp.3537-3547, 2021.
34) T. X. Dinh, T. D. Thien, T. H. V. Anh and K. K. Ahn, "Disturbance Observer Based Finite Time Trajectory Tracking Control for a 3 DOF Hydraulic Manipulator Including Actuator Dynamics," IEEE Access, Vol. 6, pp.36798-36809, 2018.